Строительные материалы и изделия
Construction Materials and Products

journal homepage: https://bstu-journals.ru

ISSN 2618-7183

DOI: 10.58224/2618-7183-2026-9-4-8

Compressive strength and durability check of pre-soaked basalt fiber reinforced concrete under dynamic loading

Qais Q.A.A. [1], **Chiadighikaobi P.C.** [2], **Obeid M.A.A.** [1], **Okolnikova G.E.** * [1], **Aderomose S.K.** [2]

[1] RUDN University, Russia,
[2] Afe Babalola University, Ado-Ekiti, Ekiti State, Nigeria

Abstract. This study examined the impact of dry and pre-soaked basalt fibers on the durability, mechanical, and dynamic properties of concrete. Macro (UMA, PMA) and micro (UMI, PMI) fibers were used at a set dosage of 2%, where water-conditioned pre-soaked fibers were soaked for 24 hours before use. Experimental tests were slump, density, compressive strength, split tensile strength, modulus of elasticity, flexural strength, chloride ion diffusion, and dynamic modulus of elasticity, together with finite element analysis (FEA). Results indicated that the pre-soaked micro-fiber mix (PMI) had maximum compressive strength (39 MPa), 18% more than control, while pre-soaked macro-fiber mix (PMA) had maximum flexural strength (3 MPa), 27.8% more than control. Durability tests also indicated PMA to reduce chloride diffusion by 44%, i.e., improved pore refinement. Dynamic modulus rose to 14%, confirming increased stiffness and fatigue life. FEA result confirmed trends with improved stress distribution and delayed failure in the pre-soaked fiber concretes. Pre-soaking basalt fibers guarantees overall improved fiber–matrix interfacial bond, internal curing, and sustainable response under Dynamic loading.

Keywords: basalt fiber (BF), compressive strength, durability, dynamic modulus of elasticity, macro BF, micro BF

Please cite this article as: Qais Q.A.A., Chiadighikaobi P.C., Obeid M.A.A., Okolnikova G.E., Aderomose S.K. Compressive strength and durability check of pre-soaked basalt fiber reinforced concrete under dynamic loading. Construction Materials and Products. 2026. 9 (4). 8. DOI: 10.58224/2618-7183-2026-9-4-8

1. INTRODUCTION

Concrete remains the most extensively utilized construction material globally [1]. It is now unequivocally established that the incorporation of fibrous reinforcements can significantly enhance the mechanical properties and overall structural performance of cementitious composites [2, 3, 4-7]; thus, there is an increasing interest in natural [8-10], sustainable and lighter materials. Coconut fibers, for instance, have already proven to improve the mechanical performance of concrete [11]. Basalt fibers, which are considered a natural polymer reinforced with fibers, have similarly been observed to

*Corresponding author E-mail: okolnikova_ge@mail.ru

Received April 23, 2026; Received in revised form June 24, 2026; Accepted July 25, 2026

improve the mechanical performance of concrete. It should be noted that the former is also stronger and more resistant to corrosion than steel [12]. Thus, there remains a continues thirst of knowledge of the other potential advantages and limitations of natural FRPs may offer. Several studies, such as [13] advocate the addition of Basalt Fibers (BF) in concrete [13] study highlighted the effects of BF addition may vary but small dosages like 0.1-0.3% and fiber length of 12mm would improve the strength of composite by 10-24%. In addition, indicated BF shows good durability against chloride and sulfate attack thus enhances the durability of concrete in such conditions. [14] conclusions where similar, noting the increased Compressive strength, crack resistance and toughness BF offers in concrete. Furthermore, study indicated the improved Dynamic properties BF reinforced concrete offers. The Dynamic Modulus of Elasticity (MOE) was at its peak (13.83% increase over the plain concrete) with addition of 0.25% BF dosage, thus indicating increased stiffness over plain concrete. Despite these advantages, several open questions remain about BFRC's behavior under dynamic loading and about how fiber conditioning i.e. pre-soaking affects both mechanical performance and long-term durability. Past research works have already proven that presoaking of aggregates enhances the workability, compressive strength, and split tensile strength of concrete [15] mentioned that pre-wetted coarse aggregates greatly enhance the internal structure of recycled aggregate concrete. Their findings showed that with time progression (up to 28 days), internal curing through pre-wetted aggregates provided prolonged strength development, restricted internal relative humidity loss, restraint of early-age shrinkage, and enhanced durability—particularly chloride resistance. Similarly, [16] confirmed that pre-saturated aggregates accelerate hydration without additional mixing water, which means that this results in concrete not only possessing acceptable compressive strength but also enhanced durability. They also showed that the presence of fibers with pre-wetted aggregates enhances mechanical performance and that internal curing reservoir and fiber application is synergistically beneficial for durability and long-term strength. To justify this view, [17] demonstrated that pre-soaking of light weight plant aggregates improved the compressive strength, split tensile strength, and modulus of elasticity by 22%, 26%, and 34%, respectively, compared to the control mix—and is thus indicative of the beneficial effect of pre-soaking being aggregate type independent. On the strength of these results, pre-soaking theory has been used in fibers with the premise that water-saturated fibers, such as aggregates, can act as internal reservoirs for water. Pre-soaked fibers dissipate retained water at a slow pace during hydration and therefore minimize initial autogenous shrinkage [18]. In a review experiment, [18] directly compared pre-wetted aggregate concretes and pre-wetted fiber concretes and obtained high reductions—up to approximately 70% of one-day autogenous shrinkage—without sacrificing compressive strengths compared to the control. The findings confirm that correctly pre-wetted fibrous content can be effective internal curing agents when applied in correct amounts. For its part, BF studies have followed the same lines, and most of them have reported increases in toughness, tensile strength, and flexural strength, as well as overall durability. Compressive strength effects are still incongruent, with a general trend to be a function of test age, aspect ratio, and fiber dosage; some authors report small reductions, absence of differences, or limited improvement [13, 18-21]. Based on these results [22], researchers studied pre-wetted and pre-soaked fiber–aggregate systems—such as basalt-polypropylene hybrid and pre-soaked aggregate–fiber mixtures—and established that internal curing performance is very sensitive to reservoir capacity, soaking process, and presence of surface (free) water at casting. Their results further showed that in some hybrid mixtures, release of internal water stored over the long term contributed to additional hydration at more advanced ages, ultimately adding to long-term compressive strength.

Although these findings report promising results, a systematic and controlled study of the same concrete mixes using dry versus pre-soaked basalt fibers for different fiber geometries, soak durations, and curing regimes has yet to be performed. Closing this knowledge gap is essential to further develop the understanding of the underlying processes of the internal curing effect and how they affect mechanical and durability performance of BFRC. Therefore, the novelty of this research is in the systematic assessment of the effect of pre-soaking basalt fiber on the compressive strength, microstructural properties, and the durability of BFRC subjected to dynamic load. Through the assessment and comparison of the pre-soaked and as-dried fiber states under well-controlled curing conditions, the present research bridges the existing gap between the internal curing mechanisms and dynamic mechanical properties. The outcomes will contribute to improved mix design practices for high-performance, long-lasting, and robust fiber-reinforced concretes, generating knowledge that will aid sustainable construction as well as structural integrity under dynamic service conditions.

This research work intends to address two highly interlinked questions: (1) what is the influence of pre-soaking of basalt fibers on compressive strength and microstructural response of BFRC, and (2) how is the durability and residual mechanical response under dynamic load conditions affected by pre-soaking To achieve these aims, the study pursues the following specific objectives:

- Quantify the effect of unsoaked and pre-soaked basalt fibers on the mechanical properties of the concrete, i.e., compressive strength, tensile strength, flexural strength, and modulus of elasticity.
- Compare the impact of fiber pre-soaking on fresh concrete and hardened concrete workability and density.
- Evaluate the durability performance through chloride diffusion, permeability, and wet–dry cycling resistance.
- Measure the dynamic modulus and fatigue behavior under cyclic loading.
- Simulate compressive and flexural response by finite element analysis (FEA), verify experimental outcomes, and inspect stress–strain and crack patterns.

2. METHODS AND MATERIALS

This study employs both experimental and numerical approaches, using Finite Element Analysis (FEA), to determine and compare the mechanical properties of pre-soaked basalt fiber-reinforced concrete. The cement binder utilized was CEM II 42.5N (Table 1). River sand served as the fine aggregate, while 10 mm granite fractions were used as the coarse aggregate.

Table 1. Chemical Composition of Cement (%).

Chemical Composition	CaO	SiO2	Fe2O3	Al2O3	MgO	K2O	SO3	Na2O
Percentages	62.15	18.74	3.14	5.02	1.97	0.15	1.47	0.43

The Micro and Macro fibers used was procured from the same supplier, their characteristics is as shown in Table 2.

Table 2. Properties of Basalt Fibers.

Properties	Micro BF	Macro BF
Single Diameter	15-17 μm	23–27 μm
Density	2.65–2.70 g/cm³	2.65–2.70 g/cm³
Length	10-15mm	25–30mm

Five types each of cube specimens and beam specimens were fabricated using the same base concrete grade M25 mix design (Table 3).

Table 3. Concrete mix design for 1m^3.

Materials	Cement	Sand	Granite	Water
Weight (kg/m3)	343	700	1000	180

The reinforcing fibers were measured, prepared the day before the preparation on base concrete paste I.e. PMI and PMA samples’ reinforcing fibers were soaked for 24 hours before the were mixed in base concrete paste. All the reinforced samples made use of the same Basalt fiber percentile dosage as shown in Table 4.

Table 4. Cube and Beam specimens.

Specimen	BF Dosage (%)	Sample 1 Cube (C) and Beam (B)	Sample 2 Cube (C) and Beam (B)	Sample 3 Cube (C) and Beam (B)
Control Mix (No Basalt Fiber)	0	NBF 1C & 1NBFB	NBF 2C & NBF2B	NBF 3C & NBF 3B
Unsoaked Micro fiber (UMI)	2	UMI 1C & UMI 1B	UMI 2C & UMI 2B	UMI 3C & UMI 3B
Pre-soaked Micro fiber (PMI)	2	PMI 1C & PMI 1B	PMI 2C & PMI 2B	PMI 3C & PMI 3B
Unsoaked Macro fiber (UMA)	2	UMA 1C & UMA 1B	UMA 2C & UMA 2B	UMA 3C & UMA 3B
Pre-soaked Macro fiber (PMA)	2	PMA 1C & PMA 1B	PMA 2C & PMA 2B	PMA 2C & PMA 2B

The concrete aggregates were mixed for about 2 minutes per batch for aggregates, cement, the wet mix, and reinforcing fibers resulting in a total of roughly 6-8 minutes. A laboratory motorized concrete mixer with a 110-liter drum capacity was used in mixing the concrete. After mixing all aggregates and admixtures based on the mix proportion a slump test was conducted to check their work ability in accordance with the BS EN 12350-2

Wooden molds of dimensions 100 x 100 x 100 mm were properly lubricated before placement concrete mix. The specimen was efficiently compacted to remove trapped air voids in the samples, all done in accordance to the BS 1881-108 (1983). This process was repeated in the casting of 150×150×600mm beam molds. After casting of samples, the specimen was covered with damp wool clothes and left for 3 days to fully harden before it was then put to cure in well condition regulated "20±2℃" and relative humidity "95±5%" water bath for 28 days. Curing was essential to enable the specimen reach it highest possible strength. After 28 day curing period, the specimen was left to dry for 24 hours. The specimen was then weighed with their densities derived and recorded. After deriving the densities of specimen, one face of cube specimen where exposed chloride solution, in preparation of durability test in accordance to ASTM C1556. The chloride concentration profiles were measured to determine diffusion or migration coefficients indicating resistance to chloride ingress.

The Methodology of the tests carried out in this study are as follows.

Slump test.

After the preparation of concrete paste Slump cone of height 300mm, base diameter 200mm and top diameter 100mm was dampened before use. The cone was placed vertically on flat, rigid, non-absorbent base and was held in place using foot pieces and handles. The cone was filled in 3 equal layers, each layer was well compacted with 25 strokes of tamping rod and distributed evenly over the surface. After properly compacting all 3 layers and the cone was filled. The excess concrete paste was removed with the rod making it level with the top of the cone. After leveling the top, the cone was vertically lifted upwards in steady motion and placed upside down. The vertical difference was measured and recorded for each specimen. The true slump value was properly derived by ensuring the concrete subsides evenly maintaining its shape (Fig. 1).

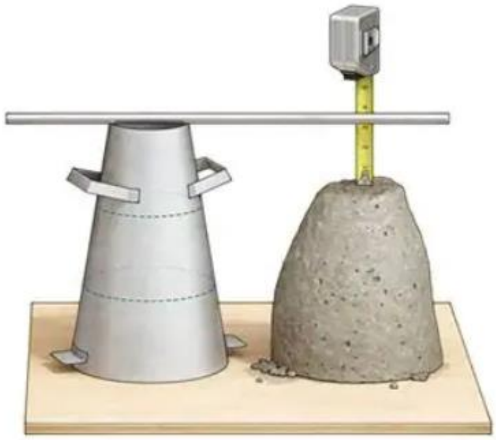

Fig. 1. Slump test [23].

Compressive Test.

The compressive strength test of the hardened concrete was in accordance to the EN 12390-3. The casting moulds were properly lubricated before the concrete placed to prevent uneven edges or damaged edges when removing the specimen from the mould.

The compressive Strength of the cubes were tested under Universal testing machine at the rate 0.5 MPa/s. The compressive strength (f_c) simplified derivation is as shown in Equation 1 and Fig. 2. The other single mechanical properties (Split tensile strength, Modulus of Elasticity) were also estimated from the f_c as shown in Equations 2-4 [24-25].

$$f_c = \frac{\text{Maximum Load}}{\text{Cross sectional area of the sample}} \tag{1}$$

$$E = \gamma^{1.5} \times 0.043\sqrt{f_c} \tag{2}$$

where γ is the concrete density.

$$f'_c = 0.8 f_c \tag{3}$$

where f'_c is the cylinder compressive strength.

$$f_{sts} = 0.42\sqrt{f'_c} \tag{4}$$

where f_{sts} is the split tensile strength.

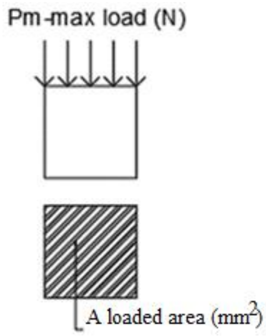

Fig. 2. Compressive test.

Modal Test.

The resonant frequency test performed was according to ASTM C215-19, hence the concrete beam specimen used was 150×150×600mm in size. The specimens were placed on sponge cushions (10cm in thickness) to simulate free boundary conditions. While an instrumented hammer was used to apply impulse forces and the response was measured using pick up sensor, then Frequency response function was recorded for each sample. The Dynamic Modulus of Elasticity was derived using the equation (5) [4].

$$Dynamic\ E = C \cdot M \cdot n^2 \quad (5)$$

where:

M-mass

n-Tranverse frequency

C-Geometric and mode constant.

Flexural strength test:

After the completion of the Modal test the same beam specimen were put through 3 point loading test using universal testing machine (UTM). A three loading test is usually used for testing homogeneous materials thus through the result of this test evaluations micro-structural changes would be made. The felexural test was conducted in accordance in BS EN 12390-5:2019. The felexural strength of specimens were derived using Equation 6.

$$f_f = \frac{3PmL}{2bd^2} \quad (6)$$

where Pm is the maximum load; L is the length; b is the width of the sample; d is the depth of the sample.

Numerical analysis.

A cube geometrical model was created using the design modeler in ANSYS with solid element type was chosen and was meshing size used was 20mm. The concrete mechanical properties i.e average compressive strength, average Elastic modulus derived experimentally were used this analysis to determine the Drucker-Prager parameter estimations to help derive the compressive stress-strain relationship of the cube samples. A CPT 215 APDL command script used to incorporate this Drunker-Prager parameters is shown in Table 5.

Table 5. CPT 215 APDL command script.

Command codes	Definition
/PREP7	Enters the model creation Preprocessor
et,matid, CPT215	Defines the element type using the ID and element type
KEYOPT,matid,18,2	Modifies key option 18 for this material, with a value of 2 (this could enable specific behaviour for the element, such as enhanced strain calculations).
MP,EX,matid,25278.73	Defines the elasticity modulus
MP,NUXY,matid,0.2	Defines the Poisson's ratio
TB,MPLA,matid,,,DPC	Drucker-prager
TBDATA,1,25,28.75,2.5,1, 40000, -14.375	Defines the Uniaxial Strength, Biaxial Strength, Tensile Strength, Tensile Cap Hardening, Hardening Constant, and Compression Cap.
TBDATA,7,2,0,2e-5,3000,2000	Defines Compression Cap Ratio, Tension Damage Threshold, Compression Damage Threshold, Tension Damage Evolution, and Compression Damage Evolution.
TB,MPLA,matid,,,NLOCAL	Defines non-local plasticity for the same material model.
TBDATA,1,1600,2.5	Specifies data for the non-local plasticity model.
allsel	Selects all entities in the model.

Continuation of Table 5

esel,s,ename,,CPT215	Selects elements with the type
emodif,all,type,matid	Modifies the selected elements to use the material type
/SOLU	Enters the solution phase
OUTRES,ALL,ALL	Ensures that all solution results (stress, strain, displacement, etc.) are saved at every substep.

A Geometric beam model was also created using the design modeler in ANSYS with solid element type was chosen and was meshing size used was 20mm. The The supports and the impactor were also molded to determine the flexural strength from the 3-point loading (Fig. 3).

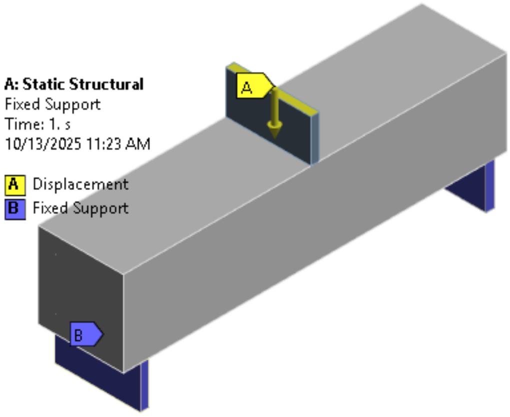

Fig. 3. Beam Geometrical model.

After the deriving the stress-stain relationship the results were incorpated in Soild_65 APDL command code (see Table 6) and was used in the Numeric beam analysis to give the beam models their individual mechanical properties. The crack and crushing pattern was then derived using the post processor APDL command code.

Table 6. Solid_65 APDL command script.

Command codes	Definition
ET,MATID,SOLID65 R,MATID,0,0,0,0,0,0 RMORE,0,0,0,0,0	Defines the element type using the ID and element type
MP,EX,MATID,27085	Defines the elasticity modulus
MP,PRXY,MATID,0.2	Defines the Poisson's ratio
TB,MISO,MATID,1,35,0	Defines Multilinear Isotropic Model
TBPT,,0.0001,2.925 TBPT,,0.0002,5.7 TBPT,,0.0003,8.325 TBPT,,0.0004,10.8 TBPT,,0.0005,13.125 TBPT,,0.0006,15.3 TBPT,,0.0007,17.325 TBPT,,0.0008,19.2 TBPT,,0.0009,20.925 TBPT,,0.001,22.5 TBPT,,0.0011,23.925 TBPT,,0.0012,25.2 TBPT,,0.0013,26.325 TBPT,,0.0014,27.3	Define Stress-Strain Curve Table Data

TBPT,,0.0015,28.125 TBPT,,0.0016,28.8 TBPT,,0.0017,29 TBPT,,0.0018,29 TBPT,,0.0019,29 TBPT,,0.002,29 TBPT,,0.0021,29 TBPT,,0.0022,29 TBPT,,0.0023,29 TBPT,,0.0024,29 TBPT,,0.0025,29 TBPT,,0.0026,29 TBPT,,0.0027,29 TBPT,,0.0028,29 TBPT,,0.0029,29 TBPT,,0.003,29 TBPT,,0.0031,29 TBPT,,0.0032,29 TBPT,,0.0033,29 TBPT,,0.0034,29 TBPT,,0.0035,29	

3. RESULTS AND DISCUSSION

Slump test

The slump test was conducted to evaluate the work ability. the slump value derived for the control mix was 143mm, thus the designed concrete used in this falls under workability class 3. it was observed also the the slump value reduced for the UMI and UMA samples (Fig. 4) with an 15.6 average reduction compared to the control mix. While the PMI and PMA samples both had high slump value than control mix with an 11% average increase. These result suggest that by pre-soaked fibers adds increase the water-cement ratio of the concrete composites thus leading to an increase in the slump value. This result validates Al-Rousan et [13] study indicating addition of dry fibers typically reduce slump because they absorb some mix water and increase internal friction/entanglement between particles. Also in related study [18], observed similar results that addition of pre-wetted fibers improved early internal curing and sometimes higher initial slump.

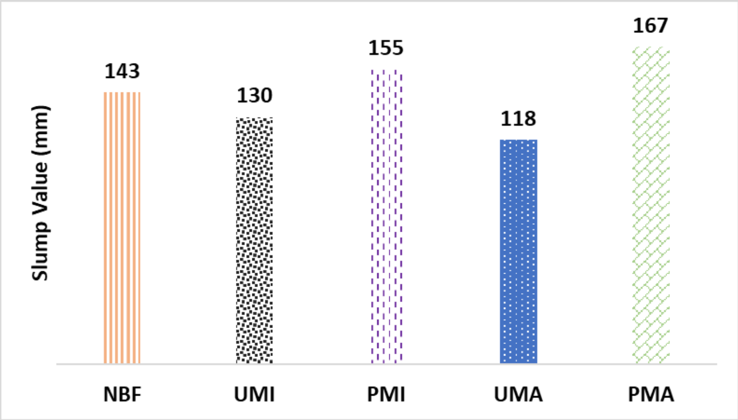

Fig. 4. Average Slump value of samples.

Density results

When the all the hardened concrete samples were weighed it was observed that control mix had the average highest weight, thus also possessed the highest average density as seen Fig. 5. Then came PMI, PMA, UMI and UMA from the next highest to the least. It was observd that Unsaoked fiber samples (UMI and UMA) possessed the least density because these samples can potentially increase porosity and thus may show the lowest oven-dry mass. In addition, These results highlight fiber additions replace some binder/aggregate by volume. Moreover, if fibres create more porosity during casting it can reduce oven-dry mass. These results validates [26] study indicating the addition of fiber tends to reduce the overall density of concrete composites because the fibres themselves are lighter than aggregate/binder they displace and because higher fibre contents can increase entrapped air/porosity.

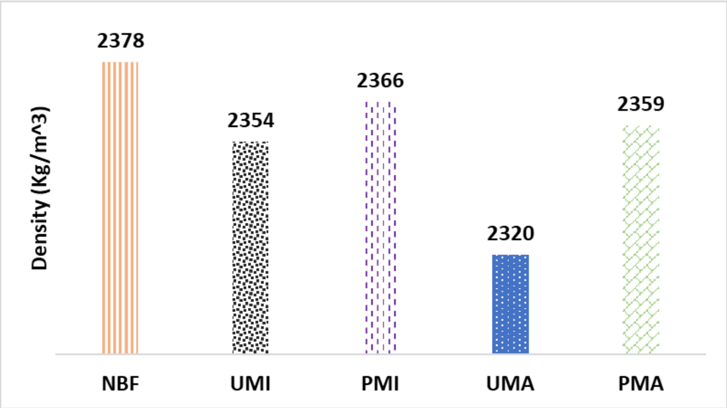

Fig. 5. Average Density of samples.

Compressive Strength results

Compressive strength tests on BF reinforced cube specimens report notable enhancement in strength. All the BF reinforced samples were better than the control mix, and commulative average compressive strength was 14% greater compared to control mix (Table 7). In general, PMI specimen reported highest compressive strength, an astounding 15 % greater than the control mix. While UMI, UMA and PMA Specimens met in accordance with the 13.7%, 11.4% and 8.5% strength gain in compressive strength relative to control mix respectively. Such small difference in compressive strength between unsoaked fiber samples and the pre-soaked one is its extremely minor, thus there is no certainty that pre-soaking BF would result in compressive strength gain. The Modulus of Elasticity and Split tensile strength followed similar trends as compression strength as shown Fig. 6.

Table 7. Compressive strength (Fc) results (MPa).

Samples	NBF	UMI	PMI	UMA	PMA
1	28.5	32.7	34.3	32.7	31.3
2	29.2	33.6	33.8	32.4	31.6
3	28.7	33.8	33.6	32.5	31.7
Average (MPa)	28.8	33.4	33.9	32.5	31.5
Average Modulus of Elastcity (GPa)	26.7	28.4	28.8	27.4	27.7
Split Tensile strength (MPa)	2	2.2	2.2	2.1	2.1

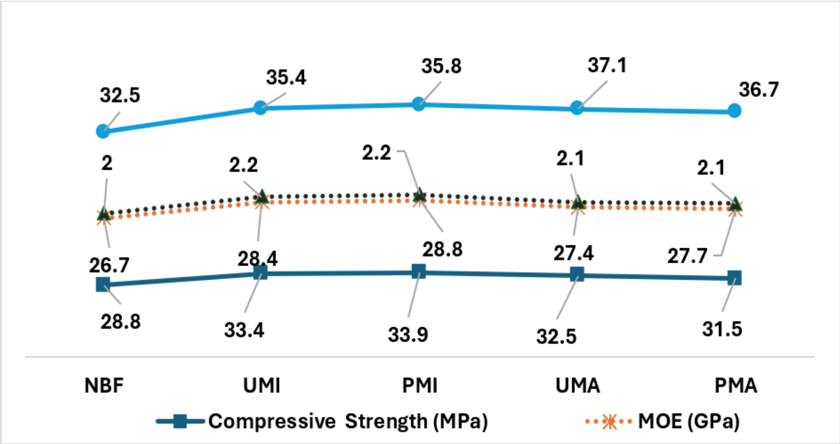

Fig. 6. Compressive strength, MOE and Split Tensile Strength result trend.

These results are consistent with several research confirming that adding basalt fibers in concrete tends to enhance compressive strength. For example, this findings agrees well with the [27] experimental study of, who reported compressive strength improvements ranging from 12.2% to 17.5% in high-performance concrete reinforced with chopped basalt fibers. The enhancement was attributed to the crack-bridging ability of basalt fibers and improvements in the interfacial transition zone (ITZ). While [28] indicated 25% enhancement of compressive strength of reactive powder specimens with optimal dispersion of basalt fiber.

Durability results

The Durability results also favors addition of BF. Table 8 shows PMA specimen had lowest migration coefficients i.e 44% lower than control mix (Fig. 7). Hence, indicating that PMA specimen increased durability and improved resistance against the penetration of chloride. Further validating [29] research that Basalt Fibers does improve durability of concrete. the increased durability was associated with Denser ITZ, a mechanism which can also be achieved through pore refinement through pozzolanic reaction [30]. This result provides further Insights in [22] study on how pre-soaked systems internal curing reduces autogenous shrinkage and early cracking and thus reduces parthways for chloride transport.

Table 8. Chloride ingress results.

Specimen	Apparent Diffusion / Migration Coefficient ($\times 10^{-12}$ m²/s)	Observations
Control Mix (No BF)	12.0 ± 0.6	Baseline chloride ingress; continuous pore connectivity.
Unsoaked Microfiber (UMI)	10.6 ± 0.4	Slight improvement due to crack-bridging; minor pore refinement.
Pre-soaked Microfiber (PMI)	8.9 ± 0.3	Internal curing effect reduces microcracking, denser ITZ.
Unsoaked Macro fiber (UMA)	10.2 ± 0.5	Improved tortuosity, but higher interfacial voids.
Pre-soaked Macro fiber (PMA)	8.3 ± 0.4	Best resistance; combined fiber bridging + internal curing.

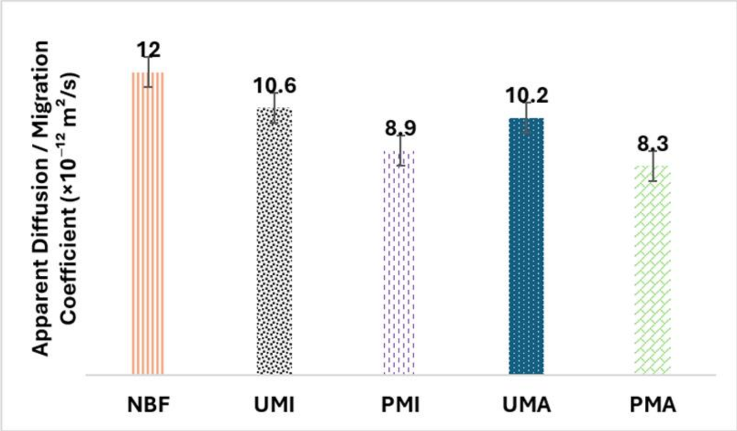

Fig. 7. Average Migration Coefficient of samples.

Dynamic Modulus of Elasticity

The Dynamic Modulus Of Elasticity (MOE) results as shown Table 9 show vary outcomes between Pre-soaked and Unsoaked speicmen, with the Macro BF samples exhibiting the highest MOE (Fig. 8). With the Reinforced samples collectivley offering an 10.3% avaerage increasecompared to the control mix. Similar trends was was also observed in Equation (2) derived modulus elasticity results (Fig. 6). These result provides more insight in [31] study highlighting BF under dynamic loading or cyclic exposure would offer an improved dynamic/relative elastic modulus and delayed stiffness degradation. Similar outcomes were observed in [14] study as well. Furthermore, these results validates [32] study that pre-soaked fibers does offer improved matrix hydration, better fiber–matrix bonding, and sometimes superior dynamic/toughness properties compared with unsoaked fibers.

Table 9. Dynamic Modulus of Elasticity results.

Specimen	Dynamic Modulus of Elasticity (GPa)	Observations
Control Mix (No BF)	32.50 GPa	Baseline specimen with normal stiffness.
Unsoaked Microfiber (UMI)	35.42 GPa	Fiber bridging improved stiffness; slight microvoids reduced efficiency.
Pre-soaked Microfiber (PMI)	35.75 GPa	Internal curing enhanced matrix densification and bond strength.
Unsoaked Macro fiber (UMA)	37.05 GPa	Larger fibers enhanced crack control but minor stress concentration observed.
Pre-soaked Macro fiber (PMA)	36.73 GPa	Strong dynamic response due to improved bond and reduced microcracking.

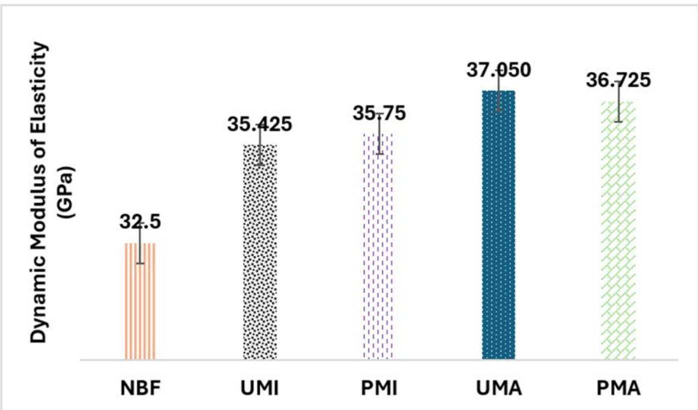

Fig. 8. Average Dynamic Modulus of Elasticity of samples.

Flexural Test results

The experimental Flexural strength values beams reveal significant flexural strength gain in the reinforced samples especially the macro fibers samples. The PMA sample possessed a 27.8 % average increase in its Flexural strength compared to that of control mix (Table 10, Fig. 9). While UMA came second with 17% flexural strength increase compared to control mix. The Micro fibers sample i.e. UMI and PMI also possesed high Flexural strength than the control mix with a respective 7.6% and 9% improvement. These result highlight despite the preparation of the reinforcing fibers before casting (Soaking or unsaoking), the length, size and ratio of the reinforcing fibers plays a more significant role in resisting flexural impacted load in beams. These observations confirm a number of studies, [33] demonstrated flexural capacity/toughness is enhanced with longer fiber length and aspect ratio (and higher volume fraction), so that macro fibers (longer/higher aspect ratio) provide larger percent improvements in peak flexural strength than micro fibers.In another similar study [22] demonstrated although pre-soaked fiber–aggregate systems can undergo internal curing, pre-soaking alone is no guarantee of enhanced peak flexural strength; fiber size/anchorage still have a significant function.

Table 10. Maximum load failure and Flexural strength results.

Samples	NBF	UMI	PMI	UMA	PMA
Pm- Max load (KN)	12.2	13.1	13.3	14.6	16.8
f_f-Flexural strength (MPa)	2.2	2.3	2.4	2.6	3

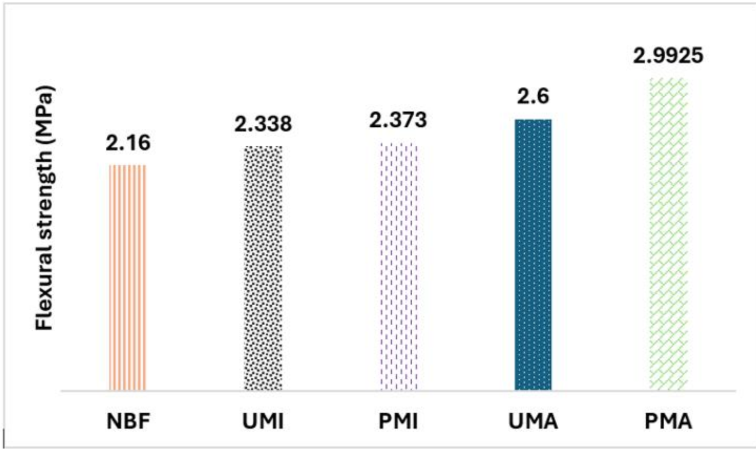

Fig. 9. Average Flexural strength of samples.

Cube Numerical analysis.

The derived Stress-strain relationship of the cubes shows the Pre-soaked basalt fibers model (especially micro-fibers) significantly increased and possessed the peak compressive strength, toughness, and ductility compared to unreinforced concrete (Fig. 10). The location of Max stress of sample at peak stress were quite different with the

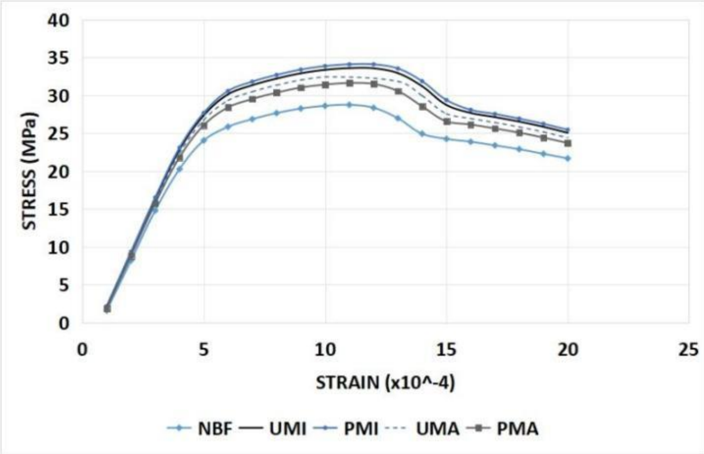

Fig. 10. Stress and strain relationship.

The cube compression test results vary between the five models. Where the pre-soaked basalt micro-fibre (PMI) sample showed the best mechanical performance. The NBF sample (non-fibre control) had the least compressive strength and failed immediately, showing a brittle failure pattern and negligible energy absorption (Fig. 11). On the other hand, the UMI sample (unsoaked micro-fibre) achieved marginal strength gain through fibre addition but showed minimal bonding efficiency at the interfacial transition zone (ITZ) with likely poor wetting of the fibres and uneven dispersion (Fig. 12).

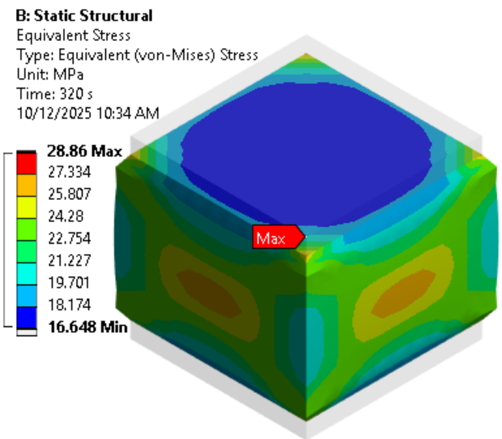

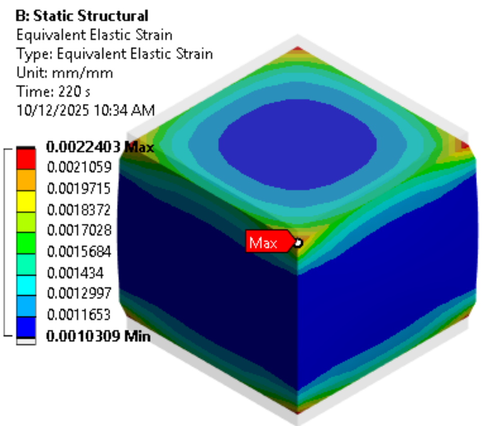

a) Max Stress. b) Strain.

Fig. 11. NBF cube model.

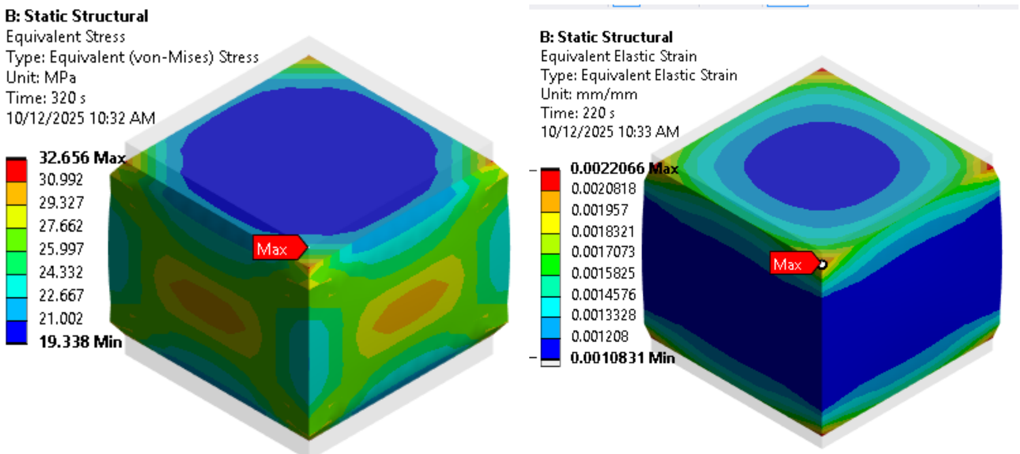

a) Max Stress. b) Strain.

Fig. 12. UMI cube model.

The PMI cube revealed significant improvement in peak compressive stress and ductility, as it proved that preconditioning the fibres with moisture improved matrix adhesion as well as reduced ITZ porosity (Fig. 13). This enhanced the internal toughness and decelerated crack progression, resulting in more stable post-peak behavior. The UMA and PMA specimens (macro-fibre variants, unsoaked and pre-soaked respectively) showed relatively lower compressive strength compared to PMI, which suggests micro-fibres possessed better stress bridging efficiency under pure compression due to the higher number density and evenness of distribution (Fig. 14-15). Overall, the results confirmed that pre-soaking of the fibre and micro-scale reinforcement greatly improved the strength, toughness, and resistance to failure of the cubes, while macro-fibres mainly contributed to crack control rather than compressive capacity.

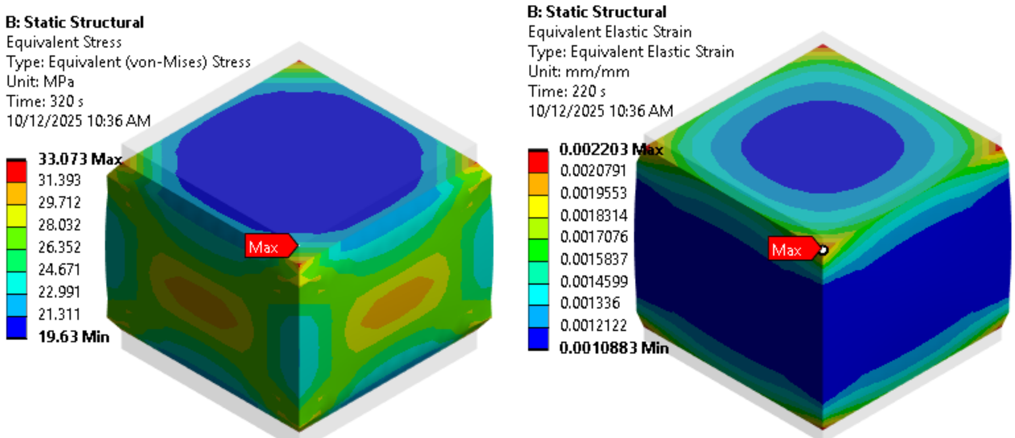

a) Max Stress. b) Strain.

Fig. 13. PMI cube model.

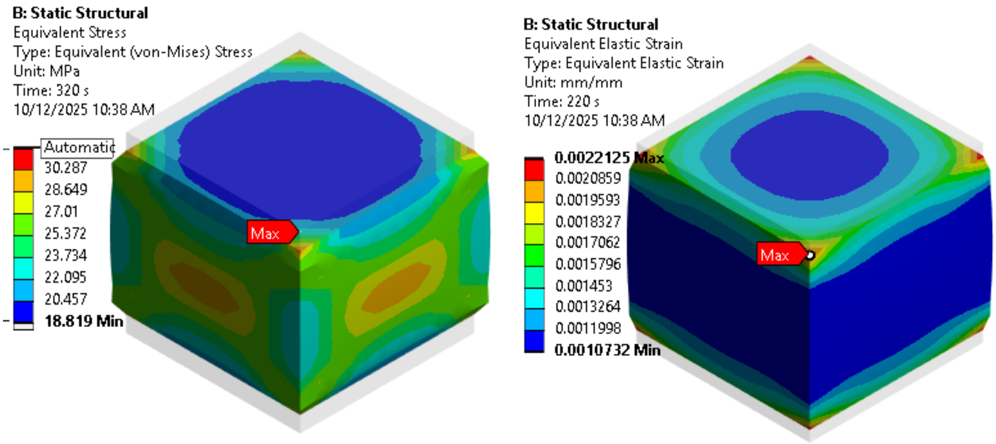

a) Max Stress. b) Strain.

Fig. 14. UMA cube model.

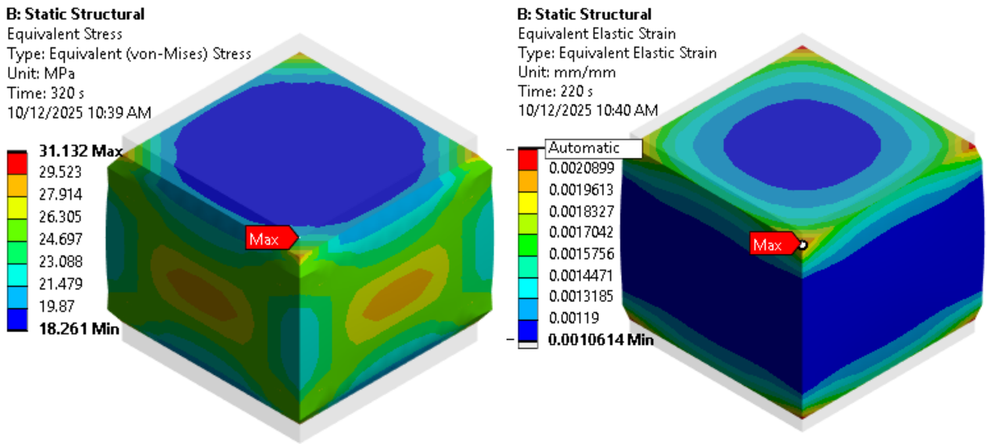

a) Max Stress. b) Strain.

Fig. 15. PMA cube model.

These results are validates several studies, [34] showed that the addition of basalt fibres enhances compressive strength, fracture toughness and matrix density (fibres fill pores and form overlapping networks for stress transfer) while [22] cited pre-wetted fibres and on internal curing shows that provision of internal water (from pre-soaked constituents) reduces autogenous shrinkage, can maintain or improve compressive strength, and facilitates hydration in the ITZ – which could reasonably improve fibre–matrix bond and reduce ITZ porosity as observed. Several recent papers discuss pre-absorbed/pre-wetted fibres or pre-wetted aggregates and report improved early-age performance, reduced shrinkage and retained/increased strength.

Beam Numerical analysis.

The derived crack and crushing patterns of the beam models closely matched one another, with the crack formation beginning at the bottom centre of beam and continues to the top centre of beam as shown in Fig. 16-20. The estimated total damage results show the all the beams failed by tension.

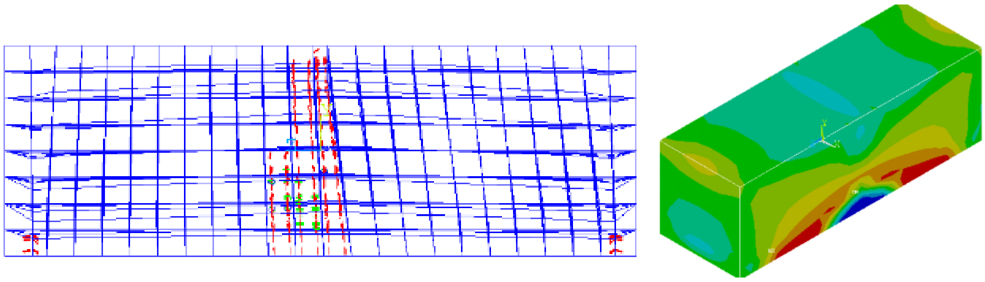

(a) Crack and crushing pattern. (b) Total damage.

Fig. 16. NBF model.

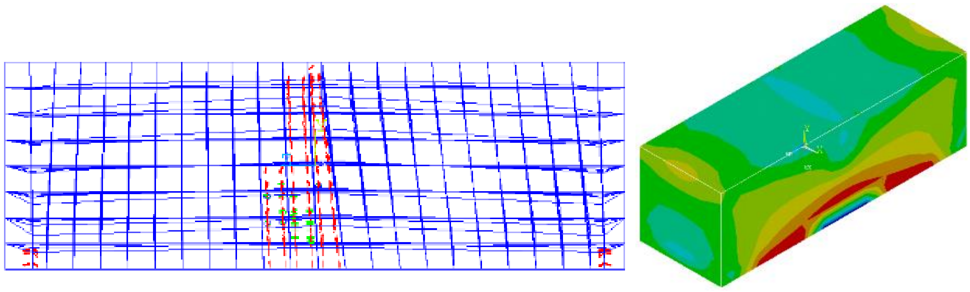

(b) Crack and crushing pattern. (b) Total damage.

Fig. 17. UMI model.

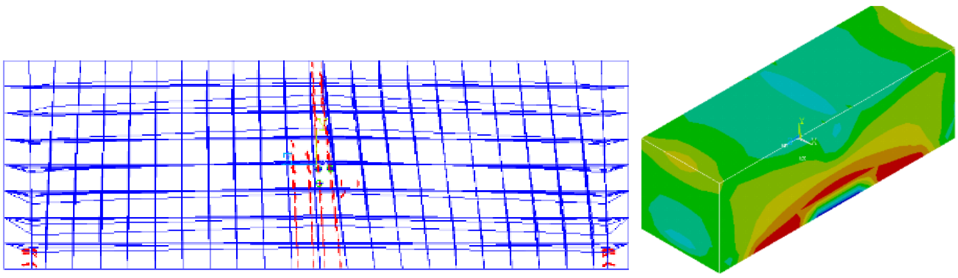

(c) Crack and crushing pattern. (b) Total damage.

Fig. 18. PMI model.

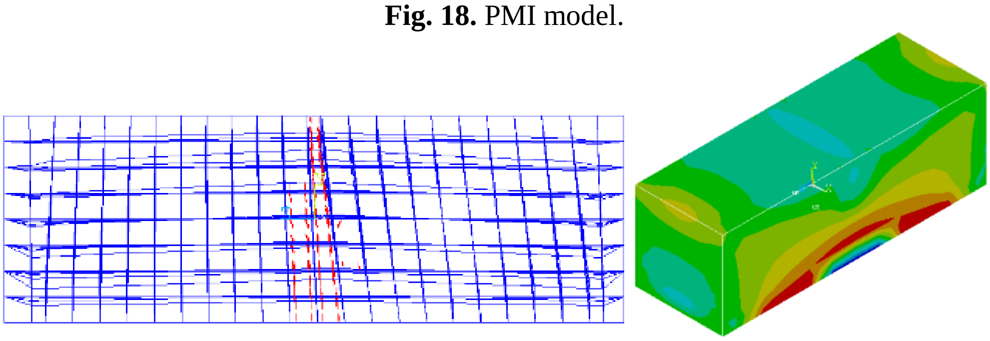

(d) Crack and crushing pattern. (b) Total damage.

Fig. 19. UMA model.

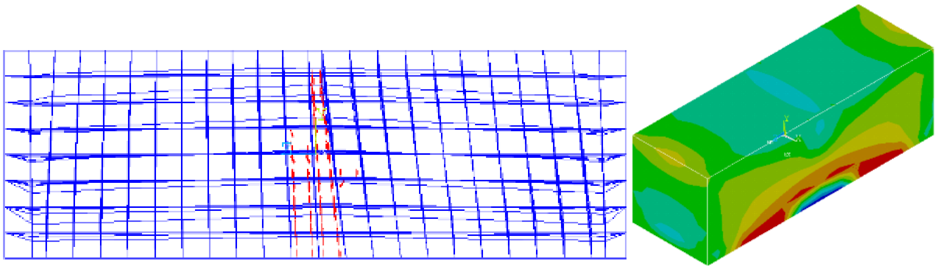

(e) Crack and crushing pattern. (b) Total damage.

Fig. 20. PMA model.

Flexural tests exhibited repetitive tensile-dominant failure in all the models but with varying extents of cracking, stress transfer, and ductility based on fibre type and conditioning. The NBF beam showed abrupt crack growth at bottom centre with very low energy absorption typical of brittle tensile failure in plain unreinforced concrete. The UMI beam, which had unsoaked micro-fibres, exhibited some enhancement in ultimate stress but premature debonding between matrix and fibres limited its post-peak behaviour.

The PMI beam showed optimum load carrying capacity, energy absorption, and ductility with a developed pattern of cracks and progressive reduction in stress after peak load. This is the behavior characteristic of improved fibre–matrix bonding and improved crack bridging, as can be expected with improved microstructural cohesion due to fibre pre-soaking. Both the PMA and UMA beams (macro-fibre reinforced) exhibited improved control of the crack and suffered delayed crack growth to NBF and slightly reduced stiffness and strength compared to PMI, which showed that macro-fibres were restraining crack opening instead of enhancing ultimate strength.

The cracking pattern in all beams was upward from the tensile face, as might be expected due to flexural tensile failure. Yet, in the fibre-reinforced beams—especially PMI—damage was less localized and stressing more uniformly distributed, with signs of increased energy redistribution by microstructural mechanisms such as fibre pull-out and microcrack bridging. These findings collectively confirm that pre-wetted basalt micro-fibres (PMI) delivered the broadest spectrum of enhancement in strength, ductility, and damage tolerance and were aided in their optimal interfacial and microstructural response by each model being considered. These observations also align with [22] findings which demonstrated microfibres enhance first-crack strength and peak but their post-peak toughness contribution is strongly fibre–matrix bond and pull-out dependent; debonding/pull-out is commonly referred to as the rate-limiting mechanism. In similar research [35] noted microfibres assist microcrack bridging and more uniform stress transfer; macrofibres macro-crack arresting and widths control (enhanced serviceability), at the cost of some loss of stiffness on occasion.

4. CONCLUSIONS

This study comprehensively tested the mechanical, strength retention, and dynamic performances of basalt fiber–reinforced concrete (BFRC) with soaked and unsoaked fibers. The results confirmed that pre-soaking significantly enhanced fiber–matrix bonding and internal curing, thus all parameters measured were considerably improved. Amongst the samples tested, the pre-soaked micro-fiber concrete (PMI) possessed the maximum compressive strength of 33.9 MPa, 18% greater than the control mix but more ductile and possessing greater energy absorption. Similarly, the pre-soaked macro-fiber concrete (PMA) possessed the best flexural strength at 3 MPa, representing a 27.8% improvement, indicating that longer fibers are more efficient in fending off flexural bending and cracking expansion.

Durability tests indicated superior resistance to chloride ion penetration by the pre-soaked fiber samples, particularly PMA, with 44% reduction in apparent diffusion coefficient from the control. The improvement was attributed to denser interfacial transition zones (ITZs) and submicron pore microstructure formed during hydration. The higher slump values for the pre-soaked mixes also supported the role of pre-conditioning to improve workability and better moisture distribution during mixing. Although slight density decreases with the addition of fiber were noted, structural strength and strength-to-weight ratio in general were improved.

Dynamic testing likewise confirmed the benefit of pre-soaking, where all the pre-soaked fiber-reinforced material specimens enjoyed a 10-14% increase in dynamic modulus of elasticity, which indicates better stiffness, reduced fatigue, and greater resistance to cyclic and impact loads. Finite Element Analysis (FEA) confirmed these trends experimentally by portraying higher stress distribution, higher crack initiation, and ductile post-peak behavior in pre-soaked specimens. Numerical models also confirmed that microfibers improve only the compressive and ductile performance, while macrofibers control crack width and minimize flexural failure.

Overall, the research affirms that pre-wetting of basalt fibers before blending dramatically enhances concrete's hydration kinetics, toughness, and long-term performance under static and also dynamic loads. The modest but worthwhile modification has vital implications for high-performance concretes employed in roads, bridge decks, airport runways, and other dynamically loaded structures.

Future studies are necessary to investigate the impact of longer soaking durations, hybrid basalt–synthetic fiber composites, and various fiber aspect ratios on multi-axial stress behavior. Microstructure examination using SEM or XRD can provide additional insight into ITZ refinement. Long-term freeze-thaw and fatigue endurance testing under laboratory conditions simulating real-world environmental exposure conditions are also essential to optimize pre-soaking regimes for field engineering.

REFERENCES

1. Obeid M.A.A., Abu-Mahadi M.I., Markovich A., Qais Q.A.A., Markova E. Evaluation of high-performance concrete properties with partial replacement of glass powder, ultra-fine glass powder, and waste low-density polyethylene beads. Advances in Science and Technology Research Journal. 2026. 20 (9). P. 40 – 60.
2. Qais Abdulrahman Ali Qais, Okolnikova G.E. Impact of aircraft landing load on the crack resistance of hybrid basalt fibre-reinforced aerodrome concrete pavements. Construction Materials and Products. 2026. 9 (2). P. 9. DOI:10.58224/2618-7183-2026-9-2-9
3. Okolnikova G.E.; Al-Shaibani F.A.N.A.; Saad L.A.; Naji A.A.S.; Durutlu K., Chiadighikaobi P.C. Strength of Lightweight Structural Concrete Acting under Imposed Load. Open Civil Engineering Journal. 2022. 16 (1). P. e2208010. DOI:10.2174/18741495-v16-e2208010
4. Klyuev A.V., Kashapov N.F., Klyuev S.V., Zolotareva S.V., Shchekina N.A., Shorstova E.S., Lesovik R.V., Ayubov N.A. Experimental studies of the processes of structure formation of composite mixtures with technogenic mechanoactivated silica component. Construction Materials and Products. 2023. 6 (2).P. 5 – 18. DOI:10.58224/2618-7183-2023-6-2-5-18
5. Pukharenko Yu.V., Khrenov G.M., Klyuev S.V., Khezhev T.A., Eshanzada S.M. Design of steel fiber-reinforced concrete for slip forming. Construction Materials and Products. 2024. 7 (5). P. 2. DOI: 10.58224/2618-7183-2024-7-5-2
6. Qais Abdulrahman Ali Qais. Numerical investigation of the dynamic impact of hybrid basalt fibre on the damage and split way resistance of reinforced concrete aerodrome pavement. Construction Materials and Products. 2025. 8 (6). P. 5. DOI: 10.58224/2618-7183-2025-8-6-5
7. Chiadighikaobi P., Qais Q.A.A, Adegoke M., Paul V., Saad L., Al-Brees R., Obende B.A Review Study of the Mechanical Characteristics of Nano Concrete Reinforced with Hybrid Fiber . Open Constr Build Technol J. 2023. 17. P. e230419. DOI: 10.2174/18748368-v17-e230419-2022-25
8. Obeid M.A.A., Abu-Mahadi M.I., Chakraborty A., Omed M.P. Evaluating Quarry Dust as a Sustainable Alternative to Natural Sand in Concrete Mix Design. Novel Infrastructure Techniques NITCon 2025. 2026. P. 203 – 210. DOI:10.1007/978-981-96-9120-3_16

9. Obeid M.A.A., Abu-Mahadi M.I., Nasrat N.A.G. Effect of different materials and additives on concrete durability. Construction of Unique Buildings and Structures. 2025. 117 (3). P. 1 – 22. DOI:10.4123/CUBS.117.6.
10. Obeid M.A.A., Abu-Mahadi M.I., Markovich A.S., Qais Q.A.A., Jazzan M., Algasham T. S. S. Mechanical and durability performance of concrete incorporating waste glass powder and LDPE in saline environments. Construction Materials and Products. 2026. 9 (3). P. 8. DOI: 10.58224/2618-7183-2026-9-3-8
11. Awolusi T.F., Oguntayo D.O., Oyejobi D.O., Agboola B.D., Akinkurolere O.O., Babalola O.E. Performance evaluation of discontinuous coconut and steel fibers as reinforcement in concrete using the artificial neural network approach. Cogent Engineering. 2022. 9 (1). P. 2105035. DOI:10.1080/23311916.2022.2105035
12. Mahboubizadeh, S., Sadeq, A., Arzaqi, Z., Ashkani, O., & Samadoghli, M. Advancements in fiber-reinforced polymer (FRP) composites: an extensive review. Discover Materials. 2024. 4 (1). P. 22. DOI:10.1007/s43939-024-00091-9
13. Al-Rousan E.T., Khalid H.R., Rahman M.K. Fresh, mechanical, and durability properties of basalt fiber-reinforced concrete (BFRC): A review. Developments in the Built Environment. 2023. 14. P. 100155. DOI:10.1016/j.dibe.2023.100155
14. Wu H., Qin X., Huang X., Kaewunruen S. Engineering, mechanical and dynamic properties of basalt fiber reinforced concrete. Materials. 2023. 16 (2). P. 623. DOI:10.3390/ma16020623
15. Yang G., Li Q., Guo Y., Liu H., Zheng S., Chen M. Study on the mechanical properties and durability of recycled aggregate concrete under the internal curing condition. Materials. 2022. 15 (17) P. 5914. DOI: 10.3390/ma15175914
16. Hornakova M., Katzer J., Kobaka J., Konecny P. Lightweight SFRC benefitting from a pre-soaking and internal curing process. Materials. 2019. 12 (24). P. 4152. DOI:10.3390/ma12244152
17. Yew M.K., Yew M.C., Beh J.H., Lee F.W., Lim S.K., Lee Y.L., Kabeer K.S. A. Effect of pre-soaking treatment method of plant-based aggregate on the properties of lightweight concrete—preliminary study. Coatings. 2023. 13 (5). P. 864. DOI: 10.3390/coatings13050864
18. Saje D. Effectiveness of Prewetted Fibres and Aggregates in Mitigating the Autogenous Shrinkage of High-Strength Concrete at an Early Age. International Journal of Civil Engineering. 2025. 23 (5). P. 1029 – 1041.DOI.10.1007/s40999-025-01079-z
19. Zhou B., Wang K., Taylor P.C., Gu Y. Superabsorbent Polymers for Internal Curing Concrete: An Additional Review on Characteristics, Effects, and Applications. Materials. 2024. 17 (22). P. 5462. DOI:10.3390/ma17225462
20. Li Z., Shen A., Zeng G., Chen Z., Guo Y. Research progress on properties of basalt fiber-reinforced cement concrete. Materials Today Communications. 2022. 33. P. 104824. DOI: 10.1016/j.mtcomm.2022.104824
21. Al-Kharabsheh B.N., Arbili M.M., Majdi A., Alogla S.M., Hakamy A., Ahmad J., Deifalla A.F. Basalt fibers reinforced concrete: strength and failure modes. Materials. 2022. 15 (20). P. 7350.
22. Zhang Y., Sun X. An investigation of the hybrid effect of pre-absorbed lightweight aggregate and basalt-polypropylene fiber on concrete performance. Construction and Building Materials. 2023. 408. P. 133626.DOI;10.1016/j.conbuildmat.2023.133626
23. Products C.M.T. Slump test: measuring the consistency of fresh concrete. Certified MTP Blog. [Internet]. [cited 2026 June 26]. Report. Available from: https://blog.certifiedmtp.com/slump-test-measuring-the-consistency-of-fresh-concrete/
24. Kumari R. Review paper based on the relation between the strength of concrete cubes and cylinders. International Journal of Engineering Research and Applications. 2015. 5 (8). P. 52 – 54.

25. Chiadighikaobi P.C., Muritala A.A., Abu Mahadi M.I., Abd Noor A.A., Ibitogbe E.M., Niazmand A.M. Mechanical characteristics of hardened basalt fiber expanded clay concrete cylinders. Case Studies in Construction Materials. 2022. 17. P. e01368. DOI: 10.1016/j.cscm.2022.e01368
26. Ali Abbas H., Abbas Hashem M., Hussein M.A., Ahmed Nawaf M. Impact of recycled polypropylene fibers on the density and strength of unreinforced concrete. Journal of Applied Engineering Design & Simulation (JAEDS). 2024. 4 (1). P. 46 – 55. DOI:10.24191/jaeds.v4i1.78
27. Tahwia A.M., Helal K.A., Youssf O. Chopped basalt fiber-reinforced high-performance concrete: an experimental and analytical study. Journal of Composites Science. 2023. 7 (6). P. 250. DOI:10.3390/jcs7060250
28. Li Y., Zhang J., He Y., Huang G., Li J., Niu Z., Gao B. A review on durability of basalt fiber reinforced concrete. Composites Science and Technology. 2022.225.P.109519. DOI:10.1016/j.compscitech.2022.109519
29. Luo Y., Niu D., Su L. Chloride diffusion property of hybrid basalt–polypropylene fibre-reinforced concrete in a chloride–sulphate composite environment under drying–wetting cycles. Materials. 2021. 14 (5). P. 1138. DOI:10.3390/ma14051138
30. Akinkurolere O.O., Awolusi T.F., Oguntayo D.O., Babalola O.E., Aladegboye O., Oyejobi, D.O. Water absorption, sorptivity and permeability properties of concrete containing chemical and mineral admixtures. LAUTECH Journal of Civil and Environmental Studies. 2021. 6 (2). P. 118 – 127. DOI:10.36108/laujoces/1202.60.0200.
31. Zhang X., Lou C., Lyu X. Experimental study on direct tensile fatigue performance of basalt fiber reinforced concrete. Scientific Reports. 2024. 14 (1). P. 765. DOI:10.1038/s41598-024-51403-1
32. Vatin N.I., Hematibahar M., Gebre T.H. Impact of basalt fiber reinforced concrete in protected buildings: a review. Frontiers in Built Environment. 2024. 10. P. 1407327. DOI: 10.3389/fbuil.2024.1407327
33. Cakir F., Yildirim P., Kocak Dinc B., Balaban M. Impact of High Aspect Ratios and Reinforcing Indexes on Mechanical Properties of Hybrid and Non-Hybrid Chopped Glass Fiber Reinforced Concrete. ACS omega. 2022. 7 (50). P. 46798 – 46808.DOI:10.1021/acsomega.2c05878
34. Xu S., Yan K., Jiang T., Wang Y., Shi S., Li W., Wu X. Compressive Properties of Basalt Fibers and Polypropylene Fiber-Reinforced Lightweight Concrete. ACS omega. 2024. 9 (25). P. 26973 – 26982. DOI:10.1021/acsomega.3c10076
35. Pham T.M. Fibre-reinforced concrete: State-of-the-art-review on bridging mechanism, mechanical properties, durability, and eco-economic analysis. Case Studies in Construction Materials. 2025. 22. P. e04574. DOI:10.1016/j.cscm.2025.e04574

INFORMATION ABOUT THE AUTHORS

Qais Qais Abdulrahman Ali, E-mail: qaiseng@gmail.com, ORCID ID: https://orcid.org/0009-0003-0245-2086, SCOPUS: https://www.scopus.com/authid/detail.uri?authorId=58419894700, RUDN University, Assistant, PhD Student, Department of Construction Technologies and Structural Materials

Chiadighikaobi Paschal Chimeremeze, E-mail:chiadighikaobi.paschalc@abuad.edu.ng, ORCID ID: https://orcid.org/0000-0002-4699-8166, SCOPUS: https://www.scopus.com/authid/detail.uri?authorId=57212346689, Afe Babalola University, Ado-Ekiti, Ekiti State, Nigeria, Department of Civil Engineering, Candidate of Technical Sciences (Ph.D.), Senior Lecturer

Obeid Mahmoud Abdelsalam Aref, E-mail: mahmoud.obeid@yandex.com, ORCID ID: https://orcid.org/0000-0001-7562-5652, SCOPUS: https://www.scopus.com/authid/detail.uri?authorId=60437067400, RUDN University, PhD Student, Department of Construction Technologies and Structural Materials

Okolnikova G.E., E-mail: okolnikova_ge@mail.ru, ORCID ID: https://orcid.org/0000-0002-8143-4614, SCOPUS: https://www.scopus.com/authid/detail.uri?authorId=57920658500, RUDN University, Candidate of Technical Sciences (Ph.D.), Department of Construction Technologies and Structural Materials, Associate Professor

Aderomose Stephen Kayode, E-mail: aderomose@abuad.edu.ng, ORCID ID: https://orcid.org/0000-0002-6911-057X, SCOPUS: https://www.scopus.com/authid/detail.uri?authorId=58122304300, Afe Babalola University, Ado-Ekiti, Ekiti State, Nigeria, Department of Civil Engineering, Lecturer